The NIKA 2011 run: results and perspectives towards a permanent camera for the Pico Veleta observatory

M. Calvo[a], M. Roesch[b], F.-X. Désert[c], A. Monfardini[a], A. Benoit[a], P. Ade[d], N. Boudou[a], O. Bourrion[e], P. Camus[a], A. Cruciani[f], S. Doyle[d], C. Hoffmann[a], S. Leclercq[b], J. F. Macias-Perez[e], P. Mauskopf[d], N. Ponthieu[c], K. Schuster[b], C. Tucker[d] and C. Vescovi[e] for the NIKA collaboration

[a]Institut Néel, CNRS & Université Joseph Fourier, BP 166, 38042 Grenoble, France;
[b]Institut de RadioAstronomie Millimétrique, 300 rue de la Piscine, 38406 Saint Martin d'Héres, France;
[c]IPAG, Observatoire de Grenoble, BP 53, 38041 Grenoble, France;
[d]Cardiff School of Physics and Astronomy, Cardiff University, CF24 3AA, United Kingdom;
[e]Laboratoire de Physique Subatomique et de Cosmologie, Université Joseph Fourier Grenoble 1, CNRS/IN2P3, Institut Polytechnique de Grenoble, 53, rue des Martyrs, Grenoble, France;
[f]Università di Roma La Sapienza, 00185 Roma, Italy

ABSTRACT

The Néel Iram Kids Array (NIKA) is a prototype instrument devoted to millimetric astronomy that has been designed to be mounted at the focal plane of the IRAM 30 m telescope at Pico Veleta (Spain). After the runs of 2009 and 2010, we carried a third technical run in October 2011. In its latest configuration, the instrument consists of a dual-band camera, with bands centered at 150 GHz and 220 GHz, each of them equipped with 116 pixels based on Lumped Element Kinetic Inductance Detectors. During the third run we tested many improvements that will play a crucial role in the development of the final, kilopixel sized camera. In particular, a new geometry based on a Hilbert curve has been adopted for the absorbing area of the LEKIDs, that makes the detectors dual-polarization sensitive. Furthermore, a different acquisition strategy has been adopted, which has allowed us to increase the photometric accuracy of the measurements, a fundamental step in order to get scientifically significant data. In this paper we describe the main characteristics of the 2011 NIKA instrument and outline some of its key features, discusse the results we obtained and give a brief outlook on the future NIKA camera which will be installed permanently on site.

Keywords: Millimeter astronomy, superconducting detectors, kinetic inductance, multiplexing, telescope, NIKA

1. INTRODUCTION

The millimetric and submillimetric regions of the electromagnetic spectrum have played a crucial role in astronomy over the last decades. Different processes taking place in the Universe emit most of their energy in this band. It is for example the case of the Cosmic Microwave Background radiation (*CMB*), the relic signal of the primordial plasma, that has been redshifted as a consequence of the expansion of the Universe and is now peaked at 2 mm. The distortion of the CMB due to the inverse Compton scattering processes that can take place when the CMB photons are propagating through the Intra Cluster Medium (*ICM*), known as Sunyaev-Zel'dovich effect , is as well concentrated in this region. In the nearby Universe, this band is of primary importance for the study of the early stages of star formation, as these take place in regions inside molecular clouds that are usually characterised by the presence of cold dust ($T \simeq 10\,\mathrm{K}$).

Due to the low energy of the photons to be observed, the developement of ultrasensitive detectors has played a crucial role in this branch of astronomy. The traditional solution is based on bolometers, detectors that

Further author information: (Send correspondence to Calvo M.)
Calvo M.: E-mail: martino.calvo@grenoble.cnrs.fr

Millimeter, Submillimeter, and Far-Infrared Detectors and Instrumentation for Astronomy VI,
edited by Wayne S. Holland, Jonas Zmuidzinas, Proc. of SPIE Vol. 8452,
845203 © 2012 SPIE · CCC code: 0277-786X/12/$18 · doi: 10.1117/12.927044

convert an incoming optical power into thermal phonons which are then measured by an appropriate thermistor. Bolometers have by now reached the Background LImited Photodedection (*BLIP*) conditions for ground based and satellite missions, meaning that their noise contribution is negligible compared to the intrinsic fluctuations of the observed flux. In this regime the only way to improve the sensitivity of an instrument is to increase the pixel count, which in turn implies the use of multiplexing techniques. If traditional bolometers are extremely difficult to implement in multiplexed readout schemes, the opposite is true for a new kind of detectors, the Kinetic Inductance Detectors (*KID*).

The KID is a pair-breaking detector based on the properties of superconductors.[1] Photon absorption is achieved when the incoming radiation has enough energy to break a Cooper Pair and create quasi-particle excitations. The subsequent variation in the density of quasi-particles, n_{qp}, induces a change in the kinetic inductance L_k of the superconductor. When the superconductor is used to make a resonating circuit, be it distributed or lumped, it is possible to measure this effect by monitoring the shift in the resonance frequency that are caused by the change in L_k.

The fundamental advantage of KID compared to traditional bolometers is that they are perfectly suited for frequency domain multiplexing. The losses in a superconductor are extremely small, what leads to very high quality factors and consequently narrow resonances. It is therefore possible to couple many detectors to one single feedline, changing their geometry in order to make them resonate at slightly different frequencies, and then read them out using an excitation signal given by the superposition of many tones, each one tuned to excite one of the resonators. This technique makes it possible to envision multiplexing factors up to one thousand or more.

The New (formerly Néel) Iram KID Array collaboration (*NIKA*) has worked since 2009 on a demonstrator instrument, designed to be mounted at the focal plane of IRAM 30 m telescope. It has been the first experiment to succesfully adopt the frequency multiplexed readout for on-sky observations, increasing its pixel count and sensitivity with each of the three technical runs, carried out in 2009,[2] 2010[3] and 2011.[4] In this paper we describe the latest setup of the NIKA camera, and the solutions that have been adopted in order to make it suitable for a permanent installation, thus acting as an ideal predecessor for the final instrument, planned to be installed on site at the end of 2014.

2. THE NIKA INSTRUMENT

At millimetric wavelengths, the atmosphere is overall very opaque, so that most of the experiments in this region of the spectrum have to be carried out on satellites. The cost of such missions are though very high compared to ground based instruments. Furthermore, the technical limits on spatial telescopes dimensions impact directly on their spatial resolution. For these reasons ground based telescopes, located in high and dry places and with very large apertures, constitute a fundamental counterpart to the satellite missions, providing increased spatial resolution and the ideal environment to test and validate new technologies before planning their use in space.

The IRAM telescope is located in the Pico Veleta area of the Sierra Nevada, Spain, at an altitude of 2850 m. This location is ideal to deploy the atmospheric windows centered at 2.1, 1.4, and 0.85 mm. Furthermore, with its 30 m main dish, the telescope is one of the largest facilities in the world for these wavelengths. Coupling a kilopixel camera to it would therefore provide the astronomical community with a facility with unprecedented characteristics.

The main systems which compose the instrument, namely the optical chain, the cryostat, the detectors array and the readout electronics, are described in this section.

2.1 The detectors

One of the critical steps in the design of the experiment has been the choice of the detector design. The NIKA collaboration has tested both distributed and lumped element resonators. In the first case, the resonant frequency is determined by the length of the superconducting line, with the most widespread geometry being the $\lambda/4$ resonator.[5] In a distributed KID, an antenna is needed to efficiently couple the radiation to it, which makes the fabrication process somewhat more complex, but at the same time, thanks to the added flexibility in the design, it is simple to choose whether to make the detector polarization sensitive or not. The lumped

element detectors are on the other hand made of two distinct sections, one acting as a capacitance and one as an inductance.[6] The inductance is typically a meandered line, whose dimensions are optimized in order to efficiently couple to the radiation, so that it can act as a direct radiation absorber, without the need of an antenna. The geometry originally proposed in 2008 is though sensitive to only one polarization, so the ease of fabrication came at the cost of a loss in the amount of absorbed optical power.

In the 2011 run of NIKA, we adopted a solution which conjugates the advantages of the LEKID with the ability to couple to both polarizations. This is based on a new geometry for the inductive section:[7] the meandered line has been replaced by a more complex structure, namely a third order Hilbert fractal pattern. This pattern allows us to uniformly fill the absorbing area and to guarantee at the same time an equal response to the two perpendicular polarizations.

The NIKA focal plane is equipped with two distinct detectors arrays, in order to be able to make dual-colour observations of the sky, with bands centered at 1.4 and 2.1 mm. The arrays used for the run are composed of 144 pixels regularly spaced on a 12x12 grid. The pitch between pixels is 2.3 mm, leading to a sampling of the focal plane of $1.25\,F\lambda$ and $0.75\,F\lambda$ for the two bands respectively. The fabrication has remained extremely easy thanks to the LEKID approach, and consists of a single etch process of a 20 nm thick aluminium layer, deposited on a High-Resistivity Silicon substrate. The frequency separation of the different resonances is achieved by changing the capacitive section, which is composed of a series of interdigitated fingers whose length is varied across the array. The resonances lie in the range between 1.3 and 1.6 GHz approximately.

2.2 The readout electronics

The readout is achieved using the approach described in Bourrion *et al.*[8] A Field Programmable Gate Array (*FPGA*), coupled to a Digital to Analog Converter, is used to generate a comb of frequencies in the range up to 233 MHz, whose separation is the same as the separation between the resonances. The comb is then upconverted by mixing it to a Local Oscillator carrier at the appropriate frequency. The resulting signal is fed into the cryostat using one single coaxial line, and excites the resonators. On the output line, one cryogenic preamplifier boosts the signal of all the detectors, which then is down-converted to get back to the base band where it can be acquired by an Analog to Digital Converter. The output tones are compared to a copy of the input tones kept as a reference, so that for each pixel it is possible to measure the component of the signal that is in phase (I) and in quadrature (Q) with respect to the reference. This allows to reconstruct the variations that the resonators have undergone and thus estimate the optical power shining on them.

One of the critical points remaining open in the 2009 and 2010 runs was the elaboration of a readout technique that would grant accurate photometric results. The first approach considered, based on a preliminary frequency sweep around the resonance to calibrate the detectors, suffered of systematic effects, due to the fact that, as the power incident on the detectors changed, the shape of the resonance was itself distorted, so that the original calibration became more and more approximate. Repeating the calibration after each sky scan eased the problem but didn't allow to get below 30% of relative photometric accuracy.

The new technique is based on a completely different approach, the details of which can be found in Calvo *et al.*[4] A new program implemented on the FPGA allows us to measure, for each data acquired by the control PC, both the (I, Q) values of the output signal of a resonator and the variations $(\delta I_{LO}, \delta Q_{LO})$ that these value undergo for a known variation of the carrier frequency given by the Local Oscillator, that is constantly modulated. This process allows to always have a reference value, to which the variation induced by a change in optical power $(\Delta I, \Delta Q)$ can be compared in order to estimate the corresponding shift in the resonance frequency. Although this process is itself dependent on the background load conditions, the fact that the $(\delta I_{LO}, \delta Q_{LO})$ are measured for each point ensures us that the reference value is constantly updated, so that the photometric accuracy is consequently better, as we show in section 3.

2.3 The optics

The overall optics system is similar to the one described in Monfardini *et al.*[3] The mirrors external to the cryostat and the corrugated lenses are the same, so that the optical characteristics such as beam profile and maximum resolution have remained unchanged. The main difference is due to the development of the dual-polarization sensitive detectors. To fully deploy the intrinsic advantage of the new geometry, we changed the filter stack on

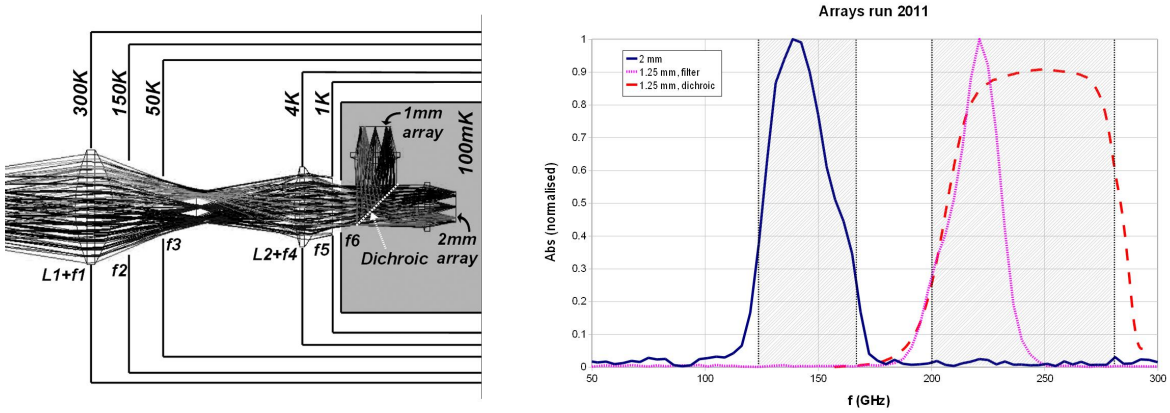

Figure 1. On the left, the optical path inside the cryostat is shown, together with a schematic representation of the different cryostat shields. L1, L2 and the lenses in front of the arrays (not marked for reasons of clarity) are all made of corrugated high density polyethylene. The differente filters are, in order, IR blocks (f1, f2), IR block and $12\,\mathrm{cm}^{-1}$ lowpass (f3), $11\,\mathrm{cm}^{-1}$ lowpass (f4) and $10\,\mathrm{cm}^{-1}$ lowpass (f5). The dichroic (f6) reflects the radiation in the band $6 \div 9\,\mathrm{cm}^{-1}$, which is sent to the 1 mm array. The rest of the radiation passes through the dichroic. To correctly define the band for the 2 mm channel, a $3.9 \div 5.7\,\mathrm{cm}^{-1}$ bandpass filter is mounted in front of the array. On the right, the resulting normalized transmission spectra. It is evident the improvement obtained by replacing the wrong lowpass filter used during the October 2011 run.

the different stages. The beam splitting between the two bands is no longer achieved by a grid polarizer, that we used in preceding runs to divide the optical power at all frequencies in two, depending on its polarization. This polarizer has been replaced by a dichroic, placed at an angle of 45°, that now allows us to divide the optical power depending on its frequency: the wavelengths between 6 and $9\,\mathrm{cm}^{-1}$ are reflected towards the 1.4 mm array, placed at 90° with respect to the main optical axis, whereas the rest of the spectrum is transmitted past the dichroic, thus illuminating the 2.1 mm array. To restrict the allowed frequencies to the ones of the bands of interest and limit the optical load on the cold stages, a series of filters is added. The external screens at 300, 150 and 50 K are all equipped with IR blocking filters, whereas on the colder stages low-pass filters are mounted, cutting at $12\,\mathrm{cm}^{-1}$ on the 50 K screen, $11\,\mathrm{cm}^{-1}$ on the 4 K, and $10\,\mathrm{cm}^{-1}$ on the 1 K. In front of the arrays, polyethylene lenses are added to make the system telecentric. Finally, band-pass filters are added just before the arrays to correctly define the band and make it coincide with the atmospheric windows. An overview of the cold optics and their performances is shown in figure 1.

2.4 The cryostat

The cryostat has undergone a major change compared to the one used in the first two runs. The original solution adopted was based on a dilution regrigerator precooled with liquid helium. This is a very common approach but has some major drawbacks, especially if a permanent camera is envisioned. In fact, the cryostat always needs some liquid helium in its tank, which implies refilling every few days. This is impossible in the case of remote operation of the system, and it poses problems even in the case of locally run experiments, as access to the telescope cabin is usually restricted to the telescope maintenance time, taking place once per week.

Though similar in dimensions, the new system uses a Pulse Tube (PT) refrigerator to precool the mixture of $^3He-^4He$, thus eliminating the need of cryogens. To reach temperatures low enough to condense the mixture, a Joule-Thompson stage is added in the circuit. This is achieved by adding a small diameter capillary on the input pipe: when exiting this impedance, the mixture expands, and under the right conditions ($T \leq 7\,\mathrm{K}$) this leads to a further cooling of the gas, down to the level where condensation can take place. The new system can be easily operated from a remote station. As of now, the only steps that require a local intervention are switching on and off the PT, and adding nitrogen to the carbon trap, used to prevent impurities from getting into the mixture circuit. Both these operations are straightforward and need to be done very seldom, but the final aim is to be

able to fully remote-control the instrument. We are aready considering possible solutions, presented in section 4.

During the first runs the detectors proved to be sensitive to the magnetic field inside the cabin, due to the Earth contribution as well as to all the instrumentation present on site. In order to reduce these potential noise sources, two magnetic shields have been added: mu-metal at 300 K and a superconducting lead screen on the 4 K stage. Furthermore, the cryostat has been placed on a vibration reduction plate to suppress microphonics.

The run of October 2011 allowed us to demonstrate the cryogen free operation of the cryostat, which performed according to expectations, reaching a base operating temperature of 90 mK.

3. RESULTS

The new readout technique used proved to be very effective in improving the relative photometric accuracy. A detailed analysis of the performances of the instrument can be found in Calvo *et al.*[4] Here we give only a brief outline of the obtained results:

1. The sensitivity has been estimated by taking maps of faint point sources, namely the gravitationally lensed quasar 4C05.19, shown in figure 2. Even under poor sky conditions, we were able to get an average Noise Equivalent Flux Density of 21 mJy $s^{0.5}$ per beam for the 2.1 mm channel. The value of 140 mJy $s^{0.5}$ per beam at 1.4 mm was more severly affected by the atmosphere opacity and turbulence, as well as being limited by a wrong filter present in the optical path, so that it should be regarded as an upper limit rather than a real estimation of sensitivity. In fact, simply replacing the wrong filter allowed us to gain a lot in terms of sensitivity: the preliminary analysis of the data taken during the last technical run, which took place in May 2012, with the filter replaced, show an improvement of about a factor three in the performances of the 1.4 mm array, so that it is now comparable to the best instruments based on bolometers and operating under similar conditions (e.g. MAMBO-2 at the 30-m telescope).

2. The relative photometric accuracy as been lowered to sligthly below 10% for both channels, a factor 3 improvement compared to previous runs. This has been achieved by introducing the new readout technique based on the $(\delta I_{LO}, \delta Q_{LO})$ method, which proved very effective.

3. The absolute photometric accuracy, measured by comparing the flux observed from sources previously measured by the IRAM Plateau de Bure interferometer, is of order of 10%.

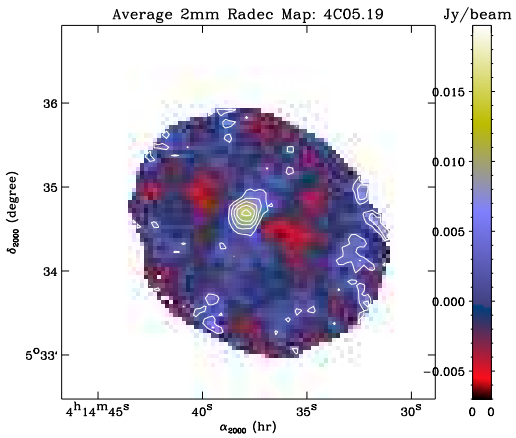

Figure 2. The 2 mm map of the gravitationally lensed quasar 4C05.19. The map has been obtained with 7 consecutive on-the-fly scans on the source, for a total of approximately 1500 s of integration.

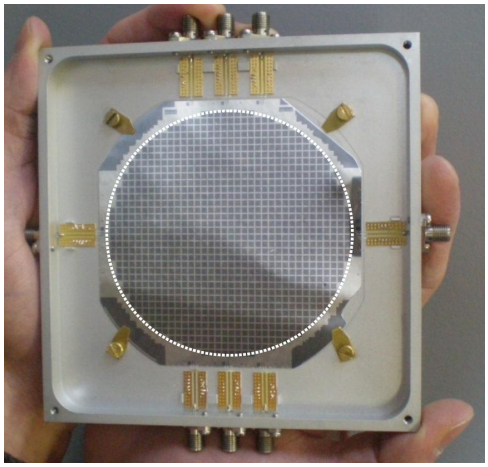

Figure 3. Image of the first 1000 pixels array fabricated for the final NIKA camera. The detectors are LEKID with an Hilbert pattern inductor, optimized for the 2.1 mm band. Four different feedlines are used to excite the detectors. A multiplexing factor of 250 is therefore necessary, which is well within the reach of the dedicated acquisition boards being developed by the NIKA collaboration. The diamater of the dotted circle is 8 cm.

4. OUTLOOK ON THE FINAL NIKA INSTRUMENT

The final aim of the NIKA project is the installation of a permanent camera at the Pico Veleta telescope that will be able to deploy the site to its maximum potential. In order to do this, we have already started to work on the upgraded instrument. One of the key aspects will be taking advantage of the large achievable focal plane. The optics chain we use today has a correct field of view of 2.8 arcmin. This is already large compared to most facilities, and yet the instrument has the potential to get a much larger mapped area. A completely new optics chain is being developed within the collaboration, which will yield a correct field of view as large as 6.5 arcmin, more than a factor 2 increase in diameter and a factor 5 in covered area. This, in turn, implies a factor 5 larger mapping speed, provided the focal plane is fully sampled.

Considering the aperture of the telescope and assuming a sampling of the focal plane of $0.75\,F\lambda$ for both the 1.4 and 2.1 mm channels, this means arrays of 3000 and 1000 detectors respectively. If the best pixel sensitivity has already been demonstrated to be as good as to reach the BLIP conditions, arrays of this size will require further work for the suppression of the cross talk among pixels and for the increase of the available band covered by the FPGA. We have already produced the first 1000 pixels samples, as shown in figure 3, and better, purpose made FPGA boards are under development.[9]

Another key aspect to consider in order to make this facility available to the world-wide astronomer community is that of remote operation. As of now, the only two steps requiring a local operator are turning on and off the Pulse Tube precooler, which can be easily updated with a remotely activated switch, and the refill of the nitrogen used to cool down the trap in the $^3He - ^4He$ mixture circuit. To solve also this second issue, the proposed solution is to shift the trap inside the cryostat, so as to cool it down with the first stage of the Pulse Tube.

These two steps needed to achieve remote operation will already be implemented in the pathfinder resident camera that we installed on site during a technical run in May 2012, so as to assess their reliability.

5. CONCLUSIONS AND PERSPECTIVES

The October 2011 run at the IRAM 30 m telescope allowed us to demonstrate the improved sensitivity and photometric accuracy, and to solve some of the issues that still prevented a permanent installation of the instrument on site.

From the scientific point of view, we have demonstated Noise Equivalent Flux Densities of $140\,\mathrm{mJy\,s^{0.5}}$ per beam at 1.4 mm and $21\,\mathrm{mJy\,s^{0.5}}$ per beam at 2.1 mm. The first value is still to be ameliorated, but we have

already identified the reason of this mediocre result and replaced the filter causing the problem. In fact already the preliminary analysis of the data taken during the last run of May 2012 show an improvement of a factor about three for the 1.4 mm channel sensitivity. The 2.1 mm channel on the contrary is already sensitive enough for carrying out scientific grade missions. This values come together with an increased relative photometric accuracy which has already largely improved compared to the previous results. We are already studying the possible solutions that could be implemented to attain the 2% level envisioned for the final instrument, considering in particular the hypothesis of an added optical calibrator to be mounted inside the cryostat.

From the technical point of view, the instrument has been changed to couple it to a Pulse Tube precooler. By eliminating the need of cryogens, this makes remote and continuous operation possible. The pathfinder instrument is now on site, and will be used in the coming years both for scientific runs and to test its stability when remotely operated. A first cool down without NIKA personnel on site is planned for the coming winter, and the solutions needed to avoid the need of local operators are already under developement.

Once fully operational, the pathfinder instrument now installed at the telescope will be the ideal demonstrator to qualify the technology and optimize the performance in view of the final NIKA camera, whose commissioning is scheduled for the end of 2014.

ACKNOWLEDGMENTS

We thank Santiago Navarro, Juan Penalvez, Carsten Kramer and the whole IRAM staff for the outstanding support during the preparation, installation and the observations. Part of this work was supported by the French National Research Agency Grant No. ANR-09-JCJC-0021-01.

REFERENCES

[1] Day, P. K., LeDuc, H. G., Mazin, B. A., Vayonakis, A., and Zmudizinas, J., "A broadband superconducting detector suitable for use in large arrays," *Nature* **425**, 817 (2003).

[2] Monfardini, A., Swenson, L. J., Bideaud, A., Désert, F. X., Yates, S. J. C., Benoit, A., Baryshev, A. M., Baselmans, J. J. A., Doyle, S., Klein, B., Roesch, M., Tucker, C., Ade, P., Calvo, M., Camus, P., Giordano, C., Guesten, R., Hoffmann, C., Leclercq, S., Mauskopf, P., and Schuster, K. F., "NIKA: A millimeter-wave kinetic inductance camera," *A&A* **521**, A29 (2010).

[3] Monfardini, A., Benoit, A., Bideaud, A., Swenson, L. J., Roesch, M., Désert, F. X., Doyle, S., Endo, A., Cruciani, A., Ade, P., Baryshev, A. M., Baselmans, J. J. A., Bourrion, O., Calvo, M., Camus, P., Ferrari, L., Giordano, C., Hoffmann, C., Leclercq, S., Macias-Perez, J. F., Mauskopf, P., Schuster, K. F., Tucker, C., Vescovi, C., and Yates, S., "The new NIKA: A dual-band millimeter-wave kinetic inductance camera for the IRAM 30-meter telescope," *ApJS* **194**, 24 (2011).

[4] Calvo, M., Roesch, M., Desert, F.-X., Monfardini, A., Benoit, A., Ade, P., Boudou, N., Bourrion, O., Camus, P., Cruciani, A., Doyle, S., Hoffmann, C., Leclercq, S., Macias-Perez, J., Mauskopf, P., Ponthieu, N., Schuster, K., Tucker, C., and Vescovi, C., "Improved mm-wave photometry for kinetic inductance detectors," *Submitted to A&ASS* (2012).

[5] Mazin, B., [*PhD Thesis*], Caltech (2004).

[6] Doyle, S., Mauskopf, P., Naylon, J., Porch, A., and Duncombe, C., "Lumped element kinetic inductance detectors," *JLTP* **151**, 530 (2008).

[7] Roesch, M. et al. *In preparation* (2012).

[8] Bourrion, O., Bideaud, A., Benoit, A., Cruciani, A., Macias-Perez, J., Monfardini, A., Roesch, M., Swenson, L., and Vescovi, C., "Electronics and data acquisition demonstrator for a kinetic inductance camera," *JINST* **6**, P06012 (2011).

[9] Bourrion, O., Vescovi, C., Gallin-Martel, L., Macias-Perez, J.-F., Monfardini, A., Benoit, A., and Calvo, M., "Electronics and data acquisition for kilopixels kinetic inductance camera," *These proceedings* (2012).